

Substrate integrated waveguide bandstop filter using partial-height via-hole resonators in thick substrate

ISSN 1751-8725

Received on 15th June 2014

Accepted on 7th April 2015

doi: 10.1049/iet-map.2015.0141

www.ietdl.org

Mahbubeh Esmaeili¹, Jens Bornemann¹ ✉, Peter Krauss²

¹Department of Electrical and Computer Engineering, University of Victoria, PO Box 1700 STN CSC, Victoria, BC, Canada, V8W 2Y2

²Mician GmbH, Schlachte 21, 28195 Bremen, Germany

✉ E-mail: j.bornemann@ieee.org

Abstract: A substrate integrated waveguide (SIW) bandstop filter on thick substrate is introduced. The increased substrate height permits partial-height via holes to act as resonators whose interaction provides a wide range of possible coupling coefficients that result in wideband bandstop filters. In contrast to ridged all-metal waveguide filters, SIW filters with partial-height via holes maintain a small profile, low manufacturing cost and they can be integrated with other planar circuitry such as microstrip or coplanar waveguide. The design method of the bandstop filter relies on the well-known extracted-pole technique which allows designers to independently control the locations of reflection zeros. The parameters of the lowpass equivalent circuit of the filter are extracted and used for the initial design of the physical dimensions of the filter. The software packages μ Wave Wizard and CST are used for filter simulation and optimisation. A prototype bandstop filter is designed for a centre frequency of 10.74 GHz and a bandwidth of 1.58 GHz. Tolerance analyses demonstrate the influence of manufacturing inaccuracies on the filter performance. Good agreement between simulated and measured results confirms the reliability and robustness of the design method and its applicability to SIW technology on thick substrate.

1 Introduction

The concept of substrate integrated waveguide (SIW) has developed into a mature technology that continues to replace all-metal waveguide components in many applications [1]. Owing to its planar nature, SIW circuits have so far been limited to comparison with and substitution of H -plane waveguide components. In waveguide technology, many advantages are derived from ridged waveguides, especially in wideband filter applications [2, 3]. Although all-metal ridged waveguide filters have good insertion loss characteristics, they are bulky and are difficult to integrate into planar microwave or millimetre-wave circuits. In addition, they are relatively expensive to manufacture. SIW technology, as alternative, enables designers to produce planar circuits which can be integrated with other planar structures. They also have better insertion loss characteristics than conventional planar circuits such as microstrip or coplanar waveguide. Owing to the possible use of standard printed-circuit board facilities, manufacturing costs of SIW filters are much lower than comparable all-metal waveguide filters.

To translate the ridged waveguide principle to SIW, a ridged SIW waveguide is introduced in [4] with partial-height via holes in the centre of the SIW and common fully plated-through vias as side walls. Another ridged SIW is introduced in [5], which is similar to the structure presented in [4], with an additional metallic strip, connecting the ends of the partial-height via holes. The modified structure presented in [5] shows wider bandwidth compared with that introduced in [4]. The bandwidths of the prototyped structures in [5] are three times wider than classical rectangular waveguides or SIWs, and their sizes are reduced by half in comparison with a SIW with the same cut-off frequency. However, filter components based on SIWs with partial-height via-holes, or so-called ridged SIWs, have not been presented so far.

Therefore to demonstrate the feasibility of partial-height via holes in SIW filters, this paper presents, for the first time, the design, simulation, prototyping and measurement of a three-pole ridged SIW wideband and compact bandstop filter. In the design procedure, the partial-height via holes are selected as resonators whose interactions can produce a large variety of couplings resulting in wideband bandstop filter realisation.

2 Design procedure and simulation

The design procedure is based on the extracted pole technique which is reviewed in this section.

2.1 Extracted pole technique

The extracted-pole technique is one of the most well-known methods to realise transmission zeros (TZs) that result in a sharp roll-off in bandpass filters. The main advantage of this technique is the independent generation and control of TZs. It is first introduced in 1980 to analytically synthesize symmetric bandpass filters with finite real TZs [6]. In the synthesised lowpass prototype, the real TZs are extracted from both ends of the two-port network and realised by simple resonators separated by phase shifters. The method in [6] is extended to realise asymmetric bandpass filters as well as symmetric ones in [7]. A method presented in [8] realises an in-line bandpass filter with one or two TZs extracted at the input and output, but without using phase shifters between resonators. Instead, frequency-independent reactances at the input and output are used. This method is verified by designing several waveguide cavity filters. Macchiarella [9] obtains similar results by starting from triplets at the input and output and then carrying out a series of circuit transformations to convert the circuit into an in-line configuration. A more general extracted-pole method is introduced in [10] for synthesising in-line bandpass filters with N TZs. This method is applied to the synthesis of several low-cost bandpass H -plane waveguide filters. The method presented in [10] is also used in [11] to design a four-pole SIW bandpass filter, albeit without partial-height (ridged) via holes.

As opposed to bandpass filters, only a few papers report on extracted-pole bandstop filters. A general extracted-pole technique for synthesising bandstop filters with arbitrarily placed reflection zeros (RZs) is presented in [12]. In this method, the resonators are connected to the main line by inverters and separated by frequency-independent phase shifters in an in-line configuration. The frequency-independent phase shifters can be optimised prior

to final realisation to take into account their actual frequency dependence. Amari *et al.* [12] use their method to synthesize and prototype a third-order *E*-plane bandstop filter with three RZs above the stopband. A new band-reject element is introduced in [13] to realise broadband bandstop filters. The element is a partial-height post in an all-metal rectangular cavity. The length of the post and its offset from the waveguide centre determine the locations of TZs and the amount of coupling, respectively. This new band-reject element permits to achieve a wide range of coupling, from weak to strong and causes a broad stopband with both symmetric and asymmetric responses. A second-order waveguide bandstop filter based on this method is prototyped in [13].

2.2 Low pass equivalent circuit extraction of bandstop filter

In this section, we design a third-order ridged SIW bandstop filter with three RZs located above the stopband. In this filter, the resonators are three partial-height plated via holes in a relatively thick substrate. The resonators are separated by phase shifters and coupled to the main SIW line by inverters. The heights of the partial-height via holes and their offset from the centre of the main SIW line determine the locations of TZs and the coupling coefficients, respectively. Input and output couplings are also required for filter realisation. They are realised as inductive irises by using additional plated-through via holes.

For this design, the bandwidth, centre frequency and attenuation in the stopband are 1.58 GHz, 10.74 GHz and 32 dB, respectively. The normalised passband RZs are at normalised angular frequencies 2.4648, 3.5242 and 4.5839 using the well-known frequency conversion formula

$$s = j\Omega = \frac{f_0}{\text{BW}} \left(\frac{f}{f_0} - \frac{f_0}{f} \right) \quad (1)$$

where f_0 and BW are the centre frequency and bandwidth of the filter.

The first step is to model a ridged SIW bandstop filter with a lowpass equivalent circuit based on the extracted-pole technique presented in [12], as shown in Fig. 1. To extract the elements of the network, we need to determine the locations of the TZs.

The reflection coefficient of a bandstop filter is related to the filtering function, $C_N(\omega)$, by

$$|S_{11}|^2 = \frac{1}{1 + \varepsilon^2 C_N^2(\omega)} \quad (2)$$

The parameter ε is related to the bandstop attenuation, RL, by $\varepsilon = (10^{\text{RL}/10} - 1)^{-1/2}$. A Chebyshev filtering function is obtained from

$$C_N(\omega) = \cosh \left[\sum_{n=1}^{n=N} \cosh^{-1} \left(\frac{\omega - \frac{1}{\omega_n}}{1 - \frac{\omega}{\omega_n}} \right) \right] = \frac{P_N(\omega)}{F_{Nz}(\omega)} \quad (3)$$

where ω_n , N and N_z are the locations of RZs, number of TZs and number of finite RZs, respectively. P_n and F_{nz} are polynomials of

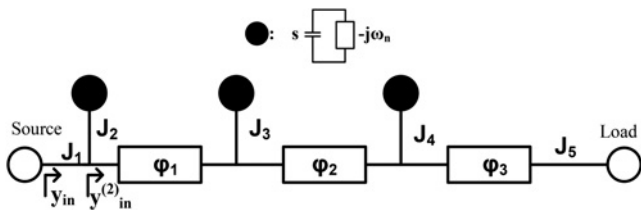


Fig. 1 Equivalent lowpass circuit for third-order extracted-pole bandstop filters according to [12]

degree N and N_z which present the numerators of S_{21} and S_{11} , respectively.

The filtering function can be calculated by a recursive formula given in [14], in rational function form. Once the filtering function is known, the denominators of S_{11} and S_{21} can be determined from the conservation of energy, that is, the unitary property of the scattering matrix.

The procedure described above calculates the filter's TZs to be located at normalised angular frequencies $\omega_1 = -0.7639$, $\omega_2 = 0.3046$ and $\omega_3 = 0.9268$. Given the locations of both RZs and TZs, the method presented in [12] is used to extract the parameters of the circuit. This method uses the reflection coefficient and input admittance to extract the filter parameters shown in Fig. 1. The reflection coefficient can be rewritten in the form

$$S_{11}(s) = e^{j\phi_{11}} \kappa \frac{\prod_{i=1}^{i=N_z} (s - s_{zi})}{\prod_{i=1}^{i=N} (s - s_{pi})} = e^{j\phi_{11}} \frac{M(s)}{D(s)} \quad (4)$$

where s_{zi} are the locations of RZs at finite frequencies and s_{pi} are S_{11} 's poles.

The phase term $e^{j\phi_{11}}$ does not affect the amplitude response of the reflection coefficient, but it is very important in the synthesis procedure. It is shown in [12] that $e^{j\phi_{11}}$ and the scaling constant κ are calculated by

$$e^{j\phi_{11}} = \frac{D(s = j\omega_1)}{M(s = j\omega_1)}, \quad \kappa^2 = \frac{\prod_{i=1}^{i=N} |j - S_{pi}|^2}{(1 + \varepsilon^2) \prod_{i=1}^{i=N_z} (1 + \omega_{zi}^2)} \quad (5)$$

If the resistance of the source is set to zero, the input impedance of the network is

$$y_{in} = \frac{1 - S_{11}(s)}{1 + S_{11}(s)} = \frac{D(s) - e^{j\phi_{11}} M(s)}{D(s) + e^{j\phi_{11}} M(s)} \quad (6)$$

On the other hand, the input impedance of the circuit in Fig. 1 is given by

$$y_{in}(s) = \frac{J_1^2}{jb_1 + (J_2^2/(s - j\omega_1)) + y_{in}^2(s)} \quad (7)$$

By equating (6) and (7) and applying the recursive formulae in [12], the parameters of the circuit shown in Fig. 1 are extracted.

Note that to start the parameter extraction procedure, we have to set the value of J_1 . Different values can be chosen depending on other inverter values between input and output. For this filter, we choose $J_1 = 1$. Then the final extracted parameters of the filter are: $J_1 = 1$, $J_2 = 1.8968$, $J_3 = 2.5620$, $J_4 = 1.3938$, $J_5 = 0.7421$, $\phi_1 = -49.0491^\circ$, $\phi_2 = -36.7040^\circ$ and $\phi_3 = -75.6224^\circ$ (c.f. Fig. 1).

2.3 Bandstop SIW filter realisation using partial-height plated via holes as resonators

In this section, we realise the extracted equivalent circuit, obtained in Section 2.2, in ridged SIW technology. The partial-height plated via holes in a thick substrate are used as resonating elements.

The initial values of the filter dimensions are obtained by relating the equivalent circuit elements to their appropriate corresponding physical parameters in the filter and force their responses to match [13]. The resonant frequencies of the resonators are mainly determined by the resonators' heights. Therefore the height of each resonator is chosen properly to bring its corresponding TZs to the desired resonant frequency. Then the coupling value J is appropriately realised by adjusting the resonator's offset from the centre of the main waveguide. Fig. 2a shows an off-centred partial-height via in rectangular waveguide, and Fig. 2b shows its equivalent T-network.

The diameter of the via is 1 mm and its offset from the centre of the waveguide is d . The waveguide is filled with RT/Duroid 6002

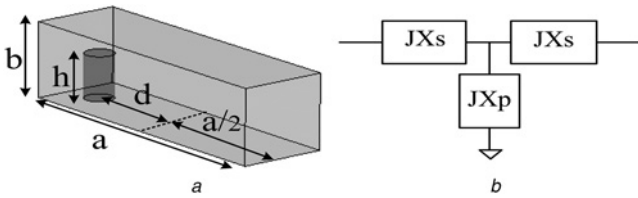


Fig. 2 Off-centred partial-height via as resonant element
a Partial-height circular via in a waveguide, $a = 10.30$ mm, $b = 3.048$ mm, $h = 2.64$ mm
b Its equivalent T-network

with dielectric constant of 2.94 and loss tangent of 0.0012. The scattering parameters of the structure shown in Fig. 2*a*, for different values of d , are presented in Fig. 3.

As shown in Fig. 3, the resonant frequency of the resonator is slightly changed by varying its offset from the centre of the waveguide. The elements of the T-network, shown in Fig. 2*b*, are extracted using scattering parameters of the resonator in Fig. 2*a* by

$$\frac{jX_p}{Z_0} = \frac{2S_{11}}{(1 - S_{11})(1 - S_{22}) - S_{12}S_{21}} \quad (8)$$

$$\frac{jX_s}{Z_0} = \frac{-2S_{11} + S_{12}S_{21} + (1 + S_{11})(1 - S_{22})}{(1 - S_{11})(1 - S_{22}) - S_{12}S_{21}}$$

As shown in Fig. 4, the series element X_s is inductive in the vicinity of the resonant frequency and almost constant. However the shunt element X_p is capacitive below the resonant frequency and inductive above it, for all different values of d .

The offset of a resonator, responsible for the normalised transmission zero ω_1 , from the centre of the waveguide is obtained by forcing the shunt element of the equivalent T-network to be

$$\frac{X_p}{Z_0} = \frac{\omega - \omega_1}{J_1^2} \quad \omega = \frac{f_0}{\text{BW}} \left(\frac{f}{f_0} - \frac{f_0}{f} \right) \quad (9)$$

$$J_1^2 = \frac{1}{\left(\frac{\partial X_p(\omega)}{\partial \omega} \right) \Big|_{\omega=\omega_1}} \quad (10)$$

The phase shifters between resonators are also realised by SIW sections with appropriate lengths. After estimating the initial values of the resonators' heights and their offsets from the main waveguide's centre, we employ the μ Wave Wizard to simulate and optimise the filter in ridged SIW technology. To facilitate low-reflection feeds in the modelling and optimisation steps, all-dielectric waveguide ports of equivalent width are used [15].

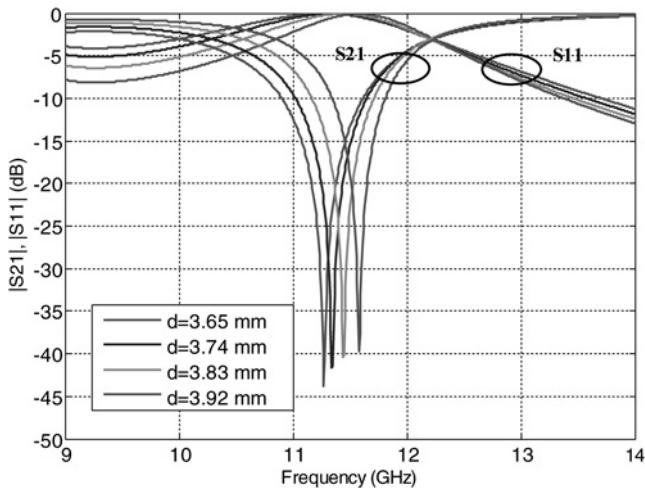


Fig. 3 Scattering parameters of the circuit shown in Fig. 2*a*

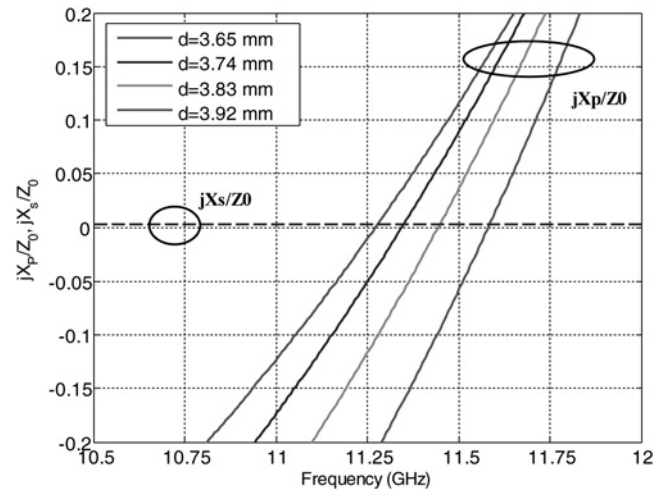


Fig. 4 Variation of equivalent circuit parameters with frequency

CST is used for verification, and the filter's three-dimensional (3D), top and bottom views in CST are shown in Figs. 5*a-c*, respectively. Fig. 6 also shows a side view of the locations of the partial-height resonators in the substrate. The substrate selected for this application is RT/Duroid 6002 with dielectric constant of 2.94, loss tangent of 0.0012, conductor thickness of $17 \mu\text{m}$ and conductivity of 5.8×10^7 S/m. The substrate thickness is 3.048 mm, because of the incorporation of partial-height vias. The diameter of all vias is 1 mm, their centre-to-centre longitudinal spacing is 1.4 mm and their lateral spacing is 11.9 mm. This leads to an equivalent waveguide width of 10.3 mm and a cutoff frequency of 8.48 GHz at the SIW ports.

Although we first chose $J_1 = 1$, during the optimisation process we have to decrease the input coupling, shown in Fig. 5*b*, to improve the passband return loss. As depicted in Fig. 7, decreasing the input coupling does not significantly change the stopband characteristics, but gives an extra degree of freedom to properly optimise the RZs' locations in the passband.

A wider frequency response of the filter is shown in Fig. 8, using μ Wave Wizard and CST. Good agreement between the two simulations confirms the integrity of the design process. As presented in Fig. 8, the cutoff frequency of the filter is 8.48 GHz which coincides with the cut-off frequency of the SIW ports (c.f. above). The designed filter creates an equi-ripple bandstop immediately after its cutoff frequency, followed by a passband extended up to the cutoff frequency of the next higher order mode at 16.96 GHz.

Note that although the designed filter has highpass application, the design process is carried out for the stopband part of the filter response using bandstop resonators. Therefore this filter can be categorised as bandstop filter with highpass application.

For comparison, the field distributions in the conventional SIW, the SIW with input and output apertures and the designed filter are presented in Fig. 9. At passband frequencies (Fig. 9*c*), the field is hardly disturbed by the partial-height via resonators. In the stopband, however, the electric fields are concentrated between the free ends of the posts and top metallic plate (Fig. 9*d*), resulting in a wide stopband.

3 Tolerances analysis of partial-height resonators

Since in the designed filter, the resonators are partial-height posts, small changes in their height can affect the filter response. Existing fabrication technologies are able to realise a partial-height via hole with $\pm 12 \mu\text{m}$ tolerances in its height. Fig. 10 shows the effects of changes, up to $\pm 12 \mu\text{m}$, of each resonator height on the transmission and reflection coefficients of the filter. As depicted in Fig. 10, any tolerances in the heights of the resonators change the attenuation in the stopband and slightly the location of the TZs, but they have no significant effect on the location of the RZs or return loss in the passband.

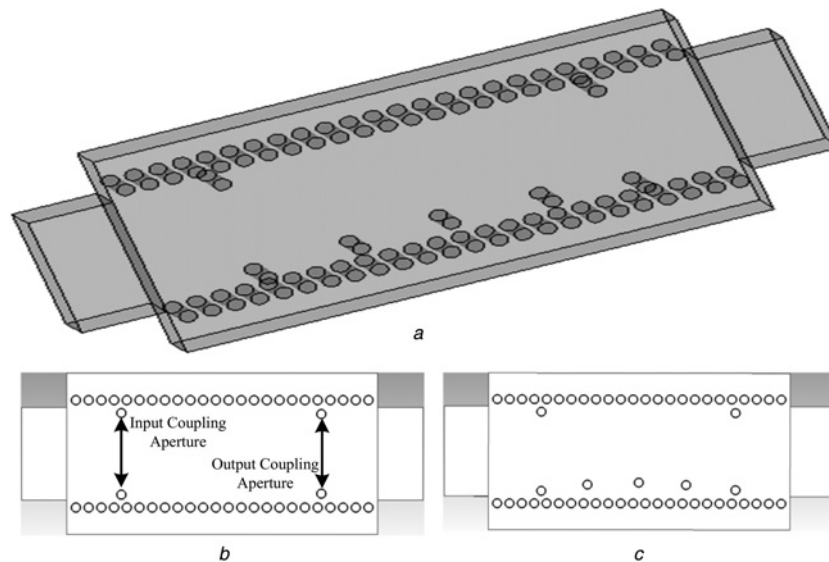


Fig. 5 Third-order ridged SIW bandstop filter with waveguide ports

a 3D view of the third-order ridged SIW filter in CST
 b Top view indicating the coupling apertures
 c Bottom view

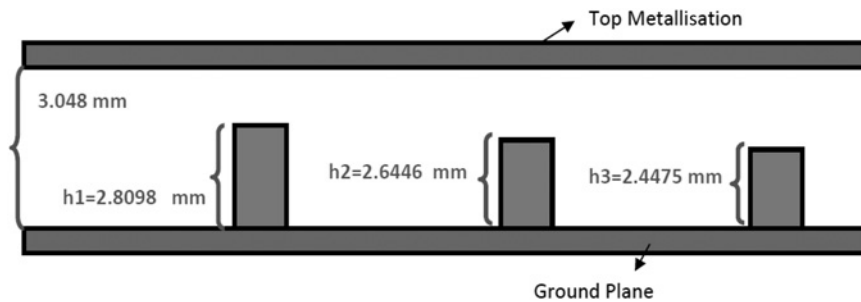


Fig. 6 Side view of the positions of the partial-height posts in a 3.048 mm substrate

4 Effects of SMA coaxial ports on bandpass and bandstop properties

For access with measurement equipment, it is common practice to use microstrip ports. Therefore the designed filter is also simulated in CST with microstrip ports. Conventional transitions to 50 Ω

microstrip are tapered lines, starting with wider width at the SIW interface and ending in the width of the 50 Ω microstrip line. For this filter, however, because of the high substrate thickness, we need to use a wider and uniform 50 Ω microstrip line, as shown in Fig. 11, that is different from conventional transitions.

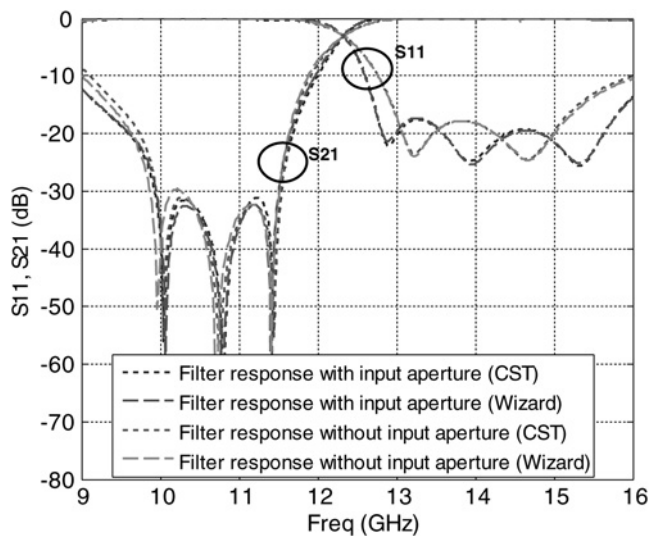


Fig. 7 Effect of input coupling on final filter response

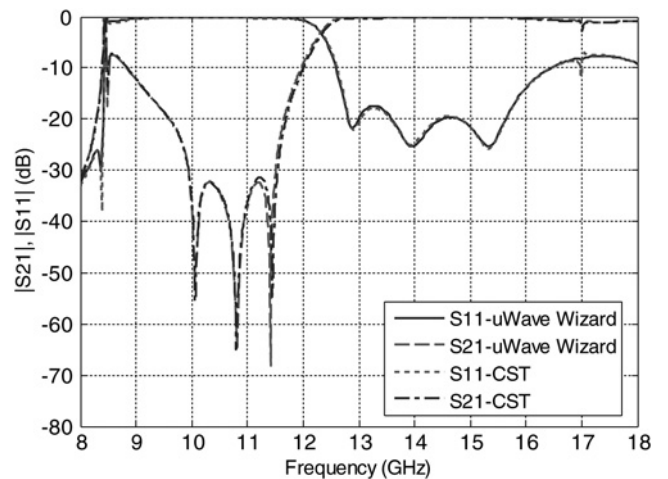


Fig. 8 Wideband simulated scattering parameters of the third-order ridged SIW filter with waveguide ports using CST and μ Wave Wizard

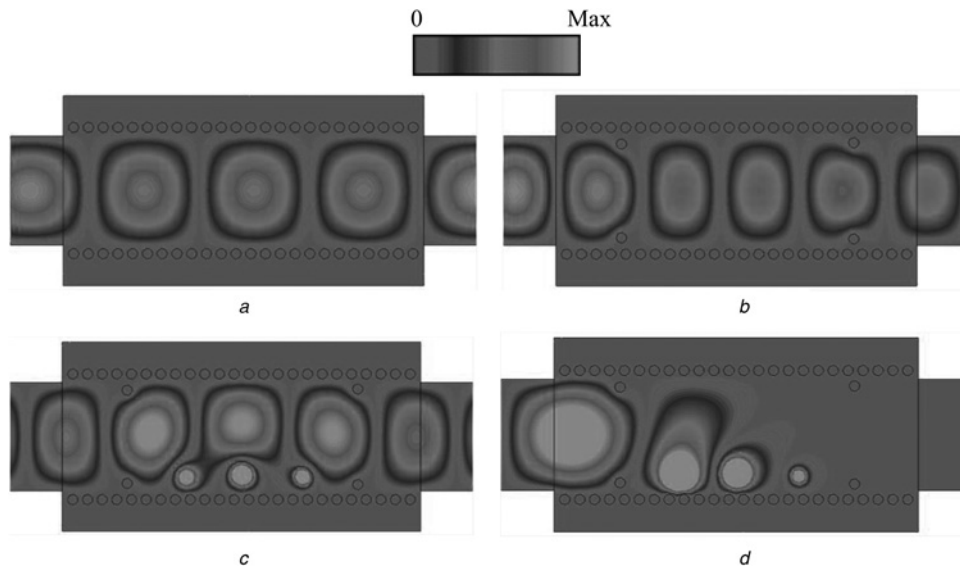


Fig. 9 Electric field distributions for
a Conventional SIW
b Conventional SIW with input and output apertures
c Designed filter at 14 GHz
d Designed filter at 10.70 GHz

On the other hand, the high substrate thickness prevents us from using a standard test fixture to measure the performance of the filter. Therefore we have to use SMA launchers to connect the vector network analyser (to the filter. Soldering coaxial SMA connectors to the wide microstrip ports may affect the responses of the filter and the measurements as the SMA launchers will have to

be connected to calibration standards as well. To reduce the influence of these connectors, the pins of the SMAs should be located exactly at the centres of the wide microstrip transitions. To investigate this effect, we simulate the filter with coaxial ports. The dimensions of the SMA connectors are chosen based on industry standards, for example [16].

Fig. 12 shows the filter responses for different ports. We observe that connecting coaxial ports to the wide microstrip transitions reduces the attenuation in the stopband and return loss in the passband. However, both values remain better than 10 dB which is acceptable for many applications.

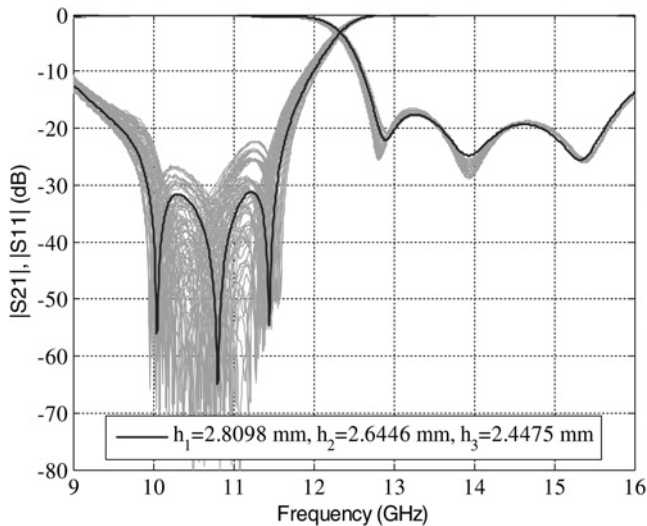


Fig. 10 Effect of changes in resonators heights on the transmission and reflection coefficients of the filter

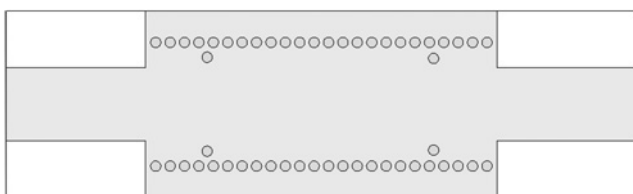


Fig. 11 Top view of the designed SIW filter with microstrip ports

5 Fabrication and experimental results

The filter designed in Section 2 is prototyped and measured. Fig. 13 shows photographs of the bottom (Fig. 13*a*) and top (Fig. 13*b*) views of the fabricated component with all its dimensions. All vias, including the partial-height resonators, are plated vias. In addition to these dimensions, the heights of the partial-height posts shown

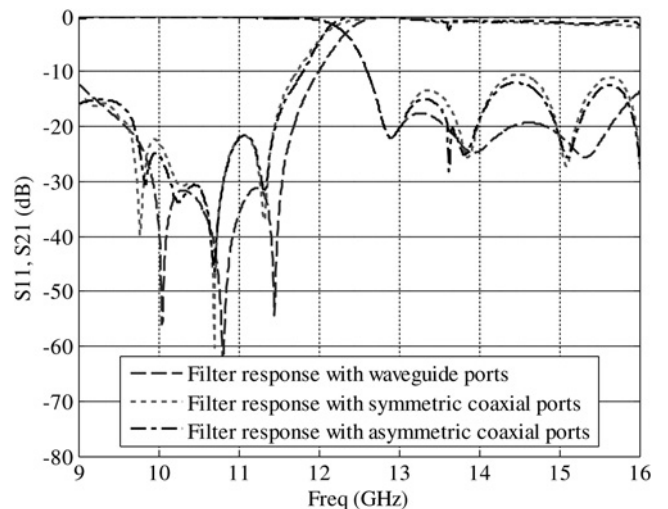


Fig. 12 Investigation of the effect of coaxial ports on the filter response

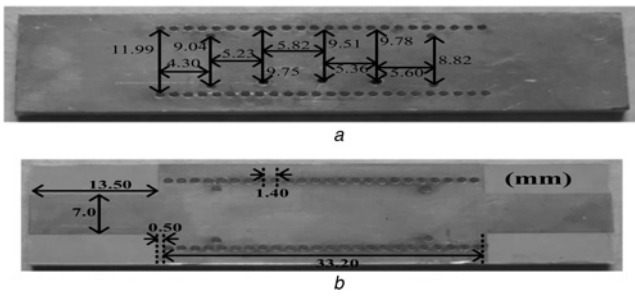


Fig. 13 Prototyped third-order ridged SIW bandstop filter with microstrip ports

a Bottom view
b Top view

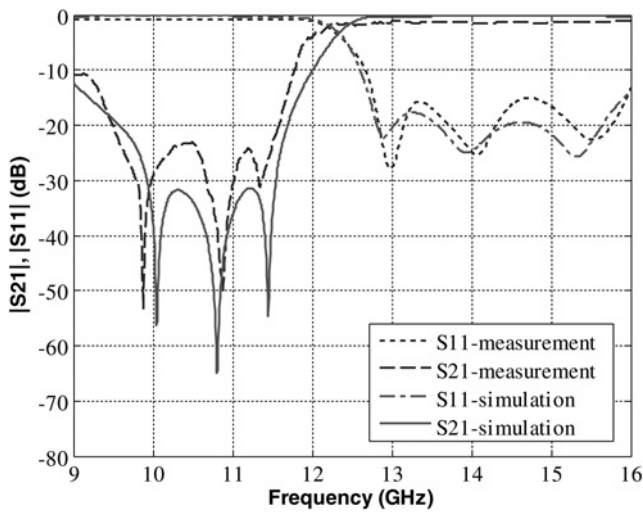


Fig. 14 Simulated and measured transmission and reflection coefficients of the third-order designed filter with microstrip ports

in Fig. 6 are $h_1 = 2.8098$ mm, $h_2 = 2.6446$ mm and $h_3 = 2.4475$ mm, from left- to right-hand side. Note again that because of the substrate thickness, the microstrip lines are wide; thus the commonly used microstrip taper section is not required.

Fig. 14 shows the comparison between simulated and measured results. A through-reflect-line calibration kit is used to deembed the effects of the microstrip transitions and soldered coaxial connectors. The measured results are in good agreement with simulations. The locations of the simulated TZs and RZs are well confirmed by measurements. The stopband attenuation is better than 20 dB, and the passband return loss is better than 12 dB up to 15.8 GHz. The maximum measured passband insertion loss is 1.8 dB at 12.68 GHz and remains below 1.5 dB between 12.68 and 15.9 GHz.

Some discrepancies in the corresponding stopband attenuation and passband return loss levels are observed. They can be attributed to the following factors. First, since in this filter, the resonators are partial-height posts in a thick, but still relatively low-profile substrate, small tolerances in the post heights can change the attenuation in the stopband as demonstrated in Section 3. Second, the tolerances of the dielectric constant, 2.94 ± 0.04 , can also affect the return loss and attenuation levels, but mainly result in a small frequency shift. Third, the effects of different (manual) soldering of coax connectors to the microstrip ports of both the filter circuit and calibration standards influence the calibration procedure and therefore measurements as shown in Section 4.

Nevertheless, the good agreement between simulation and experiment in Fig. 14 validates the design approach.

6 Conclusion

A third-order SIW bandstop (highpass) filter with partial-height via holes is synthesised, simulated, prototyped and measured. Although an all-metal ridge waveguide bandstop filter has been designed and successfully prototyped before [13], we present, for the first time, a wide stopband filter in ridged SIW technology which enables the designer to integrate it with other planar circuitry and dramatically decrease the size and reduce manufacturing costs of the filter compared with its all-metal waveguide counterpart. Good agreement between measured and simulated results demonstrates the feasibility of SIW technology with partial-height via holes and the reliability of the design method.

7 Acknowledgments

The authors thank Dr. Ralf Beyer and Dr. Thomas Sieverding, both of Mician GmbH, for helpful suggestions in modelling the ridged SIW filter. This work was supported by the TELUS Research Grant in Wireless Communications.

8 References

- 1 Wu, K.: 'State-of-the-art and future perspective of substrate integrated circuits (SICs)'. IEEE MTT-S Int. Microwave Symp. Workshop Notes: Substrate Integrated Circuits, Anaheim, USA, May 2010, pp. 1–40
- 2 Zhong Min Liu, J.A.: 'An extremely wideband ridge waveguide filter'. IEEE MTT-S Int. Microwave Symp. Digest, Fort Worth, USA, June 2004, pp. 615–618
- 3 Ruiz-Cruz, J.A., Zhang, Y., Zaki, K.A., Piloto, A.J., Tallo, J.: 'Ultra-wideband LTCC ridge waveguide filters', *IEEE Microw. Wirel. Compon. Lett.*, 2007, **17**, (2), pp. 115–117
- 4 Che, W., Li, C., Russer, P., Chow, Y.L.: 'Propagation and band broadening effect of planar integrated ridged waveguide in multilayer dielectric substrates'. IEEE MTT-S Inter. Microwave Symp. Digest, Atlanta, USA, 15–20 June 2008, pp. 217–220
- 5 Bozzi, M., Winkler, S.A., Wu, K.: 'Broadband and compact ridge substrate integrated waveguides', *IET Microw. Antennas Propag.*, 2010, **4**, (11), pp. 1965–1973
- 6 Rhodes, J.D., Cameron, R.J.: 'General extracted pole synthesis technique with application to lowpass TE₀₁₁ mode filters', *IEEE Trans. Microw. Theory Tech.*, 1980, **28**, (9), pp. 1018–1028
- 7 Cameron, R.: 'General prototype network synthesis methods for microwave filters', *ESA J.*, 1982, **6**, pp. 193–206
- 8 Amari, S., Rosenberg, U.: 'Synthesis and design of novel in-line filters with one or two real transmission zeros', *IEEE Trans. Microw. Theory Tech.*, 2004, **52**, (5), pp. 1464–1478
- 9 Macchiarella, G.: 'Synthesis of an in-line prototype filter with two transmission zeros without cross couplings', *IEEE Microw. Wirel. Compon. Lett.*, 2004, **14**, (1), pp. 19–21
- 10 Montejo-Garai, J.R., Ruiz-Cruz, J.A., Rebollar, J.M., Padilla-Cruz, M.J., Oñoro-Navarro, A., Hidalgo-Carpintero, I.: 'Synthesis and design of in-line N-order filters with N real transmission zeros by means of extracted poles implemented in low-cost rectangular H-plane waveguide', *IEEE Trans. Microw. Theory Tech.*, 2005, **53**, (5), pp. 1636–1642
- 11 Chen, X., Hong, W., Hao, Z., Wu, K.: 'Substrate integrated waveguide quasi-elliptic filter using extracted-pole technique'. Proc. Asia-Pacific Microwave Conf., Suzhou, China, December 2005, pp. 4–7
- 12 Amari, S., Rosenberg, U., Wu, R.: 'In-line pseudoelliptic band-reject filters with nonresonating nodes and/or phase shifts', *IEEE Trans. Microw. Theory Tech.*, 2006, **54**, (1), pp. 428–436
- 13 Rosenberg, U., Amari, S.: 'A novel band-reject element for pseudoelliptic bandstop filters', *IEEE Trans. Microw. Theory Tech.*, 2007, **55**, (4), pp. 742–746
- 14 Amari, S., Rosenberg, U.: 'Direct synthesis of a new class of bandstop filters', *IEEE Trans. Microw. Theory Tech.*, 2004, **52**, (2), pp. 607–616
- 15 Kordiboroujeni, Z., Bornemann, J.: 'Designing the width of substrate integrated waveguide structures', *IEEE Microw. Wirel. Compon. Lett.*, 2013, **23**, (10), pp. 518–520
- 16 Fairway Microwave, <http://www.fairviewmicrowave.com/nsearch-grid.aspx?Category=Connectors>